

# Free Streaming and Hydrodynamic Simulations of Heavy Nucleus Collisions at RHIC

M. Tilley, Arkansas State University

work done under the supervision of  
U. Heinz and P. Kolb, The Ohio State University

August 18, 2001

## Abstract

While providing excellent predictions for low  $p_{\perp}$  particle spectra and transverse radial and elliptic flow, hydrodynamic simulations of heavy nucleus collisions have disagreed with recent data on the HBT radii calculated from the collisions of Au+Au at  $\sqrt{s} = 130$  AGeV at RHIC. A novel initialization developed here to investigate the possibilities of new physics evolves the system through the process of free streaming in the pre-equilibrium phase ( $\tau < \tau_{eq}$ ). An elementary discussion of hydrodynamics, kinetic freeze-out, and HBT analysis is given, as well as the matching conditions of the free streaming initialization to the hydrodynamic evolution. Subsequent results show that for this type of initialization, freeze-out occurs approximately 13% faster with a 13% larger transverse radius. These results are better correlated with RHIC data and suggest implementation of initial free streaming may provide a reasonable approximation to the early non-equilibrium stage of the collision.

## 1 Introduction

The hydrodynamical description of heavy nucleus collisions has proven to be a highly applicable paradigm by giving a very accurate account of observables such as low  $p_{\perp}$  particle spectra in central and semi-central collisions and values for the elliptic and radial flow in semi-central collisions [1]. A recent and interesting problem for the high-energy and nuclear theory communities Hanbury-Brown-Twiss (HBT) intensity interferometry has been posed by recent measurements [2]. The values for the HBT radii,  $R_{out}$  and  $R_{side}$  from the otherwise successful hydrodynamical model do not agree with those observed in data collected by the STAR and PHENIX collaborations. It is suggested

there is some physical phenomenon occurring that is not presently included in hydrodynamical models.

We approach the problem with a novel free streaming parameterization of the initial state of the hydrodynamic evolution which effectively occurs before local thermodynamic equilibration of the collision fireball. We allow freestreaming conditions from an initial time,  $\tau_0$ , to the time of thermodynamic equilibration of the system,  $\tau_{eq}$ , and match the distribution of energy density and velocity fields from the free streaming description to the initial conditions used for the subsequent within the hydrodynamic evolution.

## 2 Introduction to Hydrodynamics

Within a hydrodynamic simulation of heavy nucleus collisions, there are three main phases of evolution: 1) pre-equilibrium, 2) hydrodynamic expansion, and 3) freeze-out of the fireball matter. New work in this paper involved developing a new initialization of the for the simulation program using a free streaming parameterization implemented during the pre-equilibrium phase. We will begin here with an elementary discussion of the existing hydrodynamic phase, and then move to a discussion of the pre-equilibrium phase in which the majority of the work was done, and finish up with a description of the freeze-out process.

The main assumption in ideal hydrodynamics is that strong interactions are occurring fast enough so that the system may be assumed to be in local thermal equilibrium, and thus be described by a local temperature  $T(x)$ , chemical potential  $\mu(x)$ , and local fluid velocity  $u^\mu(x)$ . Obviously, the system of two nuclei cannot be in thermal equilibrium the moment they collide, so there must be an interim time,  $\tau_{eq}$ , of order of the inverse collision frequency which the system requires to achieve local thermalization.

The hydrodynamic equations follow from the conservation laws for energy, momentum and net baryon density, i.e.

$$\partial_\mu T^{\mu\nu} = 0 \tag{1}$$

$$\partial_\mu j^\mu = 0, \tag{2}$$

after inserting the ideal fluid decompositions

$$T^{\mu\nu}(x) = (\epsilon(x) + P(x))u^\mu(x)u^\nu(x) - g^{\mu\nu}P(x) \tag{3}$$

$$j^\mu(x) = n(x)u^\mu(x), \tag{4}$$

where  $e(x)$  is the energy,  $P(x)$  is the pressure, and  $n(x)$  is the conserved number density at the point  $x^\mu = (t, x, y, z)$ ; the local four velocity of the fluid is given as  $u^\mu(x) = \gamma(1, v_x, v_y, v_z)$  with  $\gamma = 1/\sqrt{1 - v_x^2 - v_y^2 - v_z^2}$ .

In heavy nucleus collisions, most phenomena occur at a small angle close to the beam direction,  $z$ . The transverse plane (x,y) is perpendicular to the beam

direction. The initial energy density,  $\epsilon$ , of the ensuing fireball depends on the centrality of the collision. The impact parameter,  $b$ , is defined as the transverse distance between the centers of mass of two nuclei; it also defines the  $x$  direction in the transverse plane.

At high energies, relativistic kinematics and its influence on particle production implies longitudinal-boost invariance near midrapidity [3]. The velocity field then scales as  $v_z = z/t$  and it is convenient to describe the system using longitudinal proper time,  $\tau = \sqrt{t^2 - z^2}$  instead of  $t$ , and space-time rapidity,  $\eta = \frac{1}{2} \ln \frac{t+z}{t-z}$  instead of  $z$ . Implementing this flow profile analytically gives a reduction from (3+1)-dimensional to (2+1)-dimensional hydrodynamics in the mid-rapidity ( $\eta = 0$ ) region, which greatly simplifies the numerical calculation. In essence the longitudinally-boost invariant scheme effectively causes the absence of a longitudinal coordinate in both space-time and momentum-space coordinate systems, i.e. around  $\eta = 0$ ,  $z = p_L = 0$ . The mathematical implementation of longitudinal-boost invariance and the coordinate system transforms are given in Appendix A of [1].

## 2.1 Free Streaming

Hydrodynamics can only be considered valid when the system under consideration is in local thermal equilibrium. Therefore, there must be an input of initial conditions into the hydrodynamic code which implement the outcome of the pre-equilibrated stage. The concept of the system as a free streaming parton gas is an extreme option which is at the opposite end of the spectrum compared to the assumption of instantaneous thermalization. Free streaming shares a number of features with the other extremes of hydrodynamic evolution: the energy density is diluted, and the system expands transversally, developing a pre-equilibrium evolution into the radially outward direction akin to radial flow. Up to now, initial conditions for hydrodynamics and  $\tau_{eq}$  did not include an initial contribution transverse expansion and transverse dynamics. One rather assumed that the transverse flow at thermalization time  $\tau_{eq}$  was still zero and the transverse size still corresponded to the initial transverse overlap area of the collision nuclei. Our approach improves on this by including transverse expansion effects (both geometrically and dynamically) which have built up between  $\tau_0$  and  $\tau_{eq}$ . The concept of the system as a free streaming parton gas is one that was developed through kinetic theory for the onset of equilibrium [4]. The results of free streaming upon the system before thermal equilibration gives us a diluted energy density and something that has not been studied before, a transverse velocity field at the start of thermalization, as opposed to a later velocity field that is due to buildup of thermal pressure in the system.

To implement free streaming into the simulation, we must supply matching conditions across the boundary from a free streaming system to one that is locally thermally equilibrated and subsequently hydrodynamically expanding [5]. At equilibration time  $\tau_{eq}$  we therefore match at  $\eta=0$ , the free streaming

energy momentum tensor to the hydrodynamic energy momentum tensor,

$$T_{fs}^{\mu 0}(\mathbf{r}_\perp, \eta = 0, \tau_{eq}; \mathbf{b}) = T_{eq}^{\mu 0}(\mathbf{r}_\perp, \eta = 0, \tau_{eq}; \mathbf{b}) \quad (5)$$

with

$$T_{fs}^{\mu\nu}(\mathbf{r}_\perp, \tau_{eq}; \mathbf{b}) = \int \frac{d^3p}{E} p^\mu p^\nu f_{fs}(\mathbf{r}_\perp, \eta = 0, \tau_{eq}; \mathbf{p}_\perp, y; \mathbf{b}, \tau_0), \quad (6)$$

where  $p^\mu$ ,  $y = \frac{1}{2} \ln \frac{E+\mathbf{p}_L}{E-\mathbf{p}_L}$ , and  $f_{fs}(\mathbf{r}_\perp, \eta, \tau_{eq}; \mathbf{p}_\perp, y, \phi_p; \mathbf{b})$  are the  $\mu$ -th component of the momentum four vector, i.e.  $(E, \mathbf{p}_\perp \cos \phi_p, \mathbf{p}_\perp \sin \phi_p, \mathbf{p}_L = 0)$ , momentum-space rapidity, and the distribution function for the free streaming matter, respectively, with  $E, \mathbf{p}_\perp, \phi_p$ , and  $\mathbf{p}_L$  as the single particle energy, transverse momentum, momentum angular direction in the transverse plane, and longitudinal momentum, respectively. The free streaming distribution function [4] corresponding to boost invariant longitudinal expansion is

$$f_{fs}(\mathbf{r}_\perp, \eta, \tau_{eq}; \mathbf{p}_\perp, y, \phi_p; \mathbf{b}, \tau_0) = \frac{n_0(\tau_0)\tau_0}{\tau_{eq}} \delta(y-\eta) h(p_\perp) n_{bc}(\mathbf{r}_\perp - \frac{\mathbf{P}_\perp}{m_\perp \cosh y}(\tau_{eq}-\tau_0), \phi_r, \phi_p). \quad (7)$$

where  $n_0$  represents a normalization for reproduction of the final particle multiplicity for central collisions,

$$h(p_\perp) = e^{-p_\perp/p_s} \quad (8)$$

is the transverse momentum distribution of the initial degrees of freedom. If these are massless, the shape of  $h(p_\perp)$  turns out not to matter, and its normalization is absorbed into  $n_0$ .

$$n_{bc}(\mathbf{r}_\perp, \phi_r, \phi_p) = T_A(x + \frac{1}{2}\mathbf{b}, y) T_B(x - \frac{1}{2}\mathbf{b}, y) \quad (9)$$

represents the number of binary collisions in a differential area of the transverse plane where  $T_A$  is the nuclear thickness function of the incoming nucleus A,

$$T_A(x, y) = \int_{-\infty}^{\infty} dz \rho_A(x, y, z) \quad (10)$$

where the nuclear density  $\rho_A$  is given by a Woods-Saxon profile,

$$\rho_A(\mathbf{r}) = \frac{\rho_0}{1 + e^{(r-R_0)/\zeta}} \quad (11)$$

with  $R_0$  and  $\zeta$  representing the nuclear radius and surface diffusivity, respectively.  $n_{bc}$  gives the initial transverse density distribution of the produced particles. The delta function,  $\delta(y-\eta)$ , is included to satisfy longitudinal-boost invariance; it enforces  $\eta=0$ , where we do our matching.

Notice we only are interested in the  $\nu=0$  components of the energy-momentum tensor. This is due to the fact that we are solving only for the 3 unknowns: the

energy density and two velocity fields. Thus we do not need to make use of all of the components of the energy-momentum tensor matrix, only the three represented by  $T^{\mu 0}$ .

We assume that the initially produced, free streaming particles are massless partons. This implies  $\frac{p_{\perp}}{m_{\perp} \cosh y} = \mathbf{e}_p$ , where  $\mathbf{e}_p$  is a unit vector pointing in the direction of  $\mathbf{p}_{\perp}$ , and  $P = \frac{1}{3}\epsilon$  for the equation of state of the thermalized matter following the free streaming stage. The matching conditions can thus be written in the form

$$M^{00} = \frac{1}{3}\epsilon(4\gamma^2 - 1) \quad (12)$$

$$M^{01} = \frac{4}{3}\epsilon\gamma^2 v_x \quad (13)$$

$$M^{02} = \frac{4}{3}\epsilon\gamma^2 v_y, \quad (14)$$

where  $\epsilon$ ,  $v_x$ , and  $v_y$  correspond to the energy density, fluid velocity in the x-direction and fluid velocity in the y-direction, respectively. These matching conditions then allow us to solve for the energy density distribution and fluid velocity at each point within the collision fireball at the instant of thermalization. The matching conditions  $M^{0i}$  ( $i = 0, 1, 2$ ) above are given by the equilibrium energy-momentum tensor,

$$M^{\mu 0} = T_{eq}^{\mu 0}(\mathbf{r}, \tau_{eq}; \mathbf{b}). \quad (15)$$

The integral over  $p$  is greatly simplified by the massless parton free streaming assumption, and with partial integration over the transverse momentum term, the integral collapses into one dimension,  $\phi_p$ , which can be done numerically, i.e.

$$M^{00} = A(\tau_0) \int d\phi_p n_{bc}((\mathbf{r}_{\perp} - \mathbf{e}_p(\tau_{eq} - \tau_0); \mathbf{b})) \quad (16)$$

$$M^{01} = A(\tau_0) \int d\phi_p \cos \phi_p n_{bc}((\mathbf{r}_{\perp} - \mathbf{e}_p(\tau_{eq} - \tau_0); \mathbf{b})) \quad (17)$$

$$M^{02} = A(\tau_0) \int d\phi_p \sin \phi_p n_{bc}((\mathbf{r}_{\perp} - \mathbf{e}_p(\tau_{eq} - \tau_0); \mathbf{b})), \quad (18)$$

where

$$A(\tau_0) = \frac{n_0(\tau_0)\tau_0}{(2\pi)^3\tau_{eq}} \int_0^{\infty} dp_{\perp} p_{\perp}^3 h(p_{\perp}). \quad (19)$$

The argument of  $n_{bc}$  pertaining to the transverse position,  $\mathbf{r}_{\perp}$ , is now shifted by an amount  $\frac{\mathbf{p}_{\perp}}{m_{\perp} \cosh y}(\tau_{eq} - \tau_0) = \mathbf{e}_p(\tau_{eq} - \tau_0)$ . We implement this shift because we wish to calculate the number of binary collisions that take place at the beginning,  $\tau_0$ , of the freestreaming interval,  $\tau_{eq} - \tau_0$ ; these collisions are the

only force which drives all matter that propagated to the point  $\mathbf{r}_\perp$  during the free streaming interval, since by the massless parton free streaming assumption there are no interactions.

Once these values,  $M^{0i}$  ( $i = 0, 1, 2$ ), are obtained for each point in the transverse plane, they can be used to solve for the matching values of  $\epsilon$ ,  $v_x$ , and  $v_y$  in (12),(13), and (14). The values returned are

$$\epsilon = -M^{00} + \sqrt{(M^{00})^2 + 3((M^{00})^2 - (M^{01})^2 - (M^{02})^2)} \quad (20)$$

$$v_x = \frac{3M^{01}}{3M^{00} + \epsilon} \quad (21)$$

$$v_y = \frac{3M^{02}}{3M^{00} + \epsilon}. \quad (22)$$

For physical reasons that negative energy density cannot exist, we need to make sure that  $\epsilon$  is positive definite. Since

$$(M^{00})^2 - (M^{01})^2 - (M^{02})^2 = (M^{00})^2(1 - \langle \cos \phi_p \rangle^2 - \langle \sin \phi_p \rangle^2) \geq 0, \quad (23)$$

where

$$\langle \dots \rangle \equiv \frac{\int d\phi_p \dots n_{bc}(\mathbf{r}_\perp - \mathbf{e}_p(\tau_{\text{eq}} - \tau_0))}{\int d\phi_p n_{bc}(\mathbf{r}_\perp - \mathbf{e}_p(\tau_{\text{eq}} - \tau_0))} \quad (24)$$

is the normalized  $\phi_p$ -average over the normalized distribution  $n_{bc}$ , we can see the inequality in eqn. 23, with note that the substitution  $1 = \cos \phi_p^2 + \sin \phi_p^2$ ,

$$(\langle \cos \phi_p^2 + \sin \phi_p^2 \rangle - \langle \cos \phi_p \rangle^2 - \langle \sin \phi_p \rangle^2) = (\langle \cos \phi_p^2 \rangle - \langle \cos \phi_p \rangle^2) + (\langle \sin \phi_p^2 \rangle - \langle \sin \phi_p \rangle^2). \quad (25)$$

The values in the parentheses are the (positive definite) variances of  $\cos \phi_p$  and  $\sin \phi_p$ , so in our scheme,  $\epsilon$  is positive definite.

## 2.2 Freeze-Out

Just as free streaming occurs before hydrodynamics can be implemented, there exists later a cutoff energy density or temperature where the hydrodynamical description breaks down and kinetic freeze-out occurs. As the fireball matter expands and cools, the mean free path of the particles increases and the momentum spectra are no longer strongly affected by the scattering among the particles. Hydrodynamics is no longer valid when the average time between the scatterings approaches the expansion time scale  $\tau_{exp} = \frac{1}{\partial_\mu u^\mu}$  (inverse "Hubble constant"). It has been shown [6] that the freeze-out conditions can be well characterized by a critical constant energy density,  $\epsilon_{dec}$  or critical temperature,  $T_{dec}$ . This defines a set of space-time points, the 3-dimensional freeze-out hypersurface,  $\Sigma_f^{(i)}(x)$ .

Once the matter is diluted to the decoupling energy density, the particles stop interacting and the momenta are frozen out. This is used to calculate

the Lorentz-invariant final momentum spectra, as integrals over the freeze-out surface [7],

$$\frac{dN}{\pi dy dm_T^2} = \frac{g}{(2\pi)^3} \int_{\Sigma} d^3\Sigma_{\mu}(x) f_i(x, p) p^{\mu} \quad (26)$$

where

$$f_i(x, p) = \frac{g}{(2\pi)^3} \frac{1}{e^{[p \cdot u(x) - \mu_i(x)]/T_{dec}(x)} \pm 1}, \quad (27)$$

is the equilibrium distribution function at freeze-out, where  $g$  is the spin-isospin degeneracy factor for each particle species  $i$ .

Once all of the particle spectra are determined, they can be included in the calculation of HBT radii.

### 3 Hanbury-Brown-Twiss Radii

Analyzing data in high energy experiment is a tedious process. Experimentally, the final momentum spectra of all particles produced at the freeze-out hypersurface are recorded. Since, by the uncertainty principle, we cannot simultaneously know the position and momentum of a particle with exact precision there must be another method of extracting the positions of these particles at freeze-out using only the final momentum of the particles. This apparant miracle is possible by exploiting two-particle Bose-Einstein correlations. Their measurements provides the so called "HBT radii" which are the only known window that we have to view what phenomena are occurring in the collision fireball, which due to its small size ( $10^{-15}$  m) and short lifetime ( $10^{-23}$  s), cannot be viewed directly.

The Hanbury-Brown-Twiss effect is similar to Young's double slit experiment. Instead of interfering electromagnetic waves, though, we measure the interference of the intensity of two similar particles detected in different detectors, thus this type of interferometry is referred to as intensity interferometry. When a particle is detected in one detector with a certain momentum, the probability of detecting an identical particle in another detector is correlated to the transverse separation of the two detectors. The degree of this correlation is related to the angular diameter of the source emitting the particles. After collecting data from collisions, one looks for pairs of identical particles and constructs their 2-body correlation function. From it the HBT radii can be reconstructed to obtain an estimate of the size and lifetime of the collision fireball.

Starting point for the formalism is the general definition of the source-function (e.g. equ. (23) in [8])

$$S_{\alpha}(x, K) = \frac{2s_{\alpha} + 1}{(2\pi)^3} \int_{\Sigma} \frac{K^{\mu} d^3\sigma_{\mu}(x') \delta^4(x - x')}{\exp\{\beta(x')[K \cdot u(x') - \mu_{\alpha}(x')]\} - 1}, \quad (28)$$

for a particle of four momentum,  $K$ , and thermodynamic variables defined and denoted as usual.

First consider what this expression actually means: Integrating over all  $x$ , we recover the Cooper-Frye formula which we used above to evaluate the particle spectra (see eqn (26))

$$\int d^4x S_i(x, p) = \frac{dN}{\pi dy dm_T^2} = E \frac{dN_i}{d^3p} = \frac{g}{(2\pi)^3} \int_{\Sigma} d^3\sigma_{\mu}(x) f_i(x, p) p^{\mu} \quad (29)$$

as described e.g. in eqn. (2.11) of [1].

So this is a nice feature of the source-function, eqn. 28: It is a function defined at every space-time point  $x^{\mu}$ , but it is zero everywhere except on the freeze-out hypersurface  $\Sigma$ . This hypersurface can be given by a more or less convenient parametrization which tries to describe the system in an adequate way, or result from a more sophisticated simulation of the time evolution of the collision region (i.e. a hydrodynamic simulation). Then the freeze-out hypersurface is not given as a smooth function of the space-time coordinates, but rather sampled by little flat triangles, squares, etc. This makes the numerical evaluation of the corresponding integrals a little more involved.

In any case, we understand now that the source function tells us how a differential piece of the freeze-out hypersurface shines, in other words it gives the differential contribution to the particle spectra of this particular piece.

The HBT radii can be calculated [9] from the average emission points, that is  $\langle x \rangle$ ,  $\langle y \rangle$ ,  $\langle z \rangle$   $\langle t \rangle$  and the squares  $\langle x^2 \rangle$ , as well as mixed terms, e.g.  $\langle xt \rangle$ . These averages, or expectation values, are momentum dependent averages over the source function,

$$\langle g(x, y, z, t) \rangle := \frac{\int d^4x g(x, y, z, t) S(x, p)}{\int d^4x S(x, p)}. \quad (30)$$

The various HBT-radii are simple linear combinations of the correlation lengths  $\langle \tilde{x}_{\mu} \tilde{x}_{\nu} \rangle$ , where  $\tilde{x}_{\mu} = x_{\mu} - \langle x_{\mu} \rangle$ , evaluated at the average momentum  $K$  of the pair of identical particles:

$$R_{side}^2(K) = \langle \tilde{y}^2 \rangle(K), \quad (31)$$

$$R_{out}^2(K) = \langle (\tilde{x} - \beta_{\perp} \tilde{t})^2 \rangle(K), \quad (32)$$

The variances  $\langle x_{\mu} x_{\nu} \rangle$  characterize the space-time width of the source of the pairs with momentum  $K$ , with transverse and longitudinal pair velocities  $\beta_{\perp} = \frac{K_{\perp}}{E_K}$ ,  $\beta_L = \frac{K_L}{E_K}$ .

## 4 Discussion and results

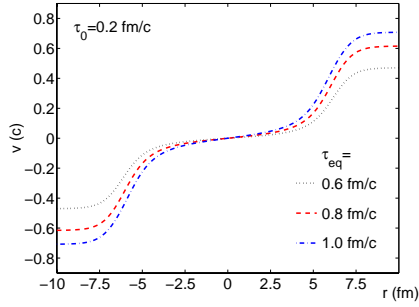


Figure 1: Initial velocity as a function of radius for the free streaming interval beginning at  $\tau_0=0.2$  fm/c to  $\tau_{eq}=0.6, 0.8,$  and  $1.0$  fm/c and the non free streaming (NFS) case.

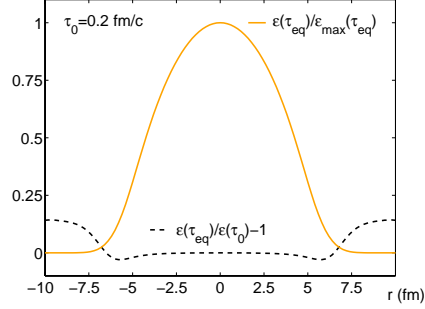


Figure 2: The energy density profile at the onset of thermalization renormalized to its maximum value,  $\epsilon(\tau_{eq})/\epsilon_{max}(\tau_{eq})$ , and the % difference between  $\epsilon(\tau_{eq})$  and  $\epsilon(\tau_0)$ .

With the free streaming scheme in place, we see some interesting new physics given in the results by the hydrodynamic model. Notice in Fig. (1), the initial velocity profiles for the fireball matter radially increased to some maximum value, which is directly proportional to the length of the interval; for greater  $\tau_{eq}$  the initial transverse flow was stronger, so the radial distance of the freeze-out hypersurface, e.g. see the profiles in Fig. (3), in the transverse plane was greater as the matter traveled a farther distance in similar amounts of time.

For central collisions,  $b = 0$ , the freeze-out hypersurface displayed a decrease of approximately 13% in lifetime and a 13% increase in radius. When the system is freestreaming, the initial energy density distribution that is passed on to the hydrodynamic expansion is lower as you extend radially from the center of the collision, shown as the percentile difference in Fig. (2), therefore the system reaches the freeze-out critical energy density,  $\epsilon_{dec}$ , at a faster rate. Similarly, the initial transverse flow, seen in Fig. (1), produced in this free streaming state causes the distribution to grow to a larger size at an earlier time, so the freeze-out hypersurface will be found at a larger radius. While all results here are shown for the initial free streaming time  $\tau_0=0.2$  fm/c, there was a comparison analysis run with  $\tau_0=0.0$  fm/c to ascertain whether any major differences would surface. The differences in the model between the  $\tau_0=0.0$  fm/c and  $\tau_0=0.2$  fm/c cases were minute, compared to the differences between the cases of no free streaming and free streaming from  $\tau_0=0.2$  fm/c, so they were not included in this work.

Figure (3) shows that in comparison with the hydrodynamic model with no free streaming (NFS), the model with free streaming implemented from  $\tau_0 = 0.2$  fm/c has an approximate 13% shorter lifetime and a 13% larger radius at freeze-out. It is interesting to note the shape of the NFS curve. Near  $\tau = 0$  fm/c, the

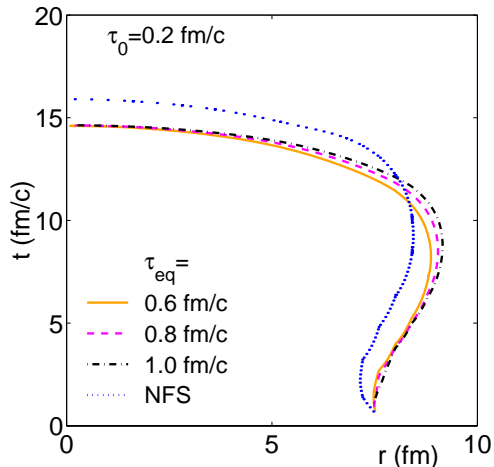


Figure 3: Profiles of the freeze-out hypersurfaces with free streaming from  $\tau_0=0.2$  fm/c to  $\tau_{eq}=0.6, 0.8,$  and  $1.0$  fm/c; also the non free streaming (NFS) case.

fireball first experiences freeze-out on the perimeter of the fireball, approx. 7.5 fm, where the particles are at the lowest  $\epsilon$ , and makes its way inward towards higher densities. After the initial cooling of the outer layer, the fireball material toward the center of the collision begins to expand in the transverse plane due to thermal energy being converted into collective motion and the freeze-out hypersurface then reverses its direction and begins growing outward to allow this highly dense internal matter to expand and cool. So the tendency of the freeze-out hypersurface for the NFS case is to begin with an inward motion, and abruptly reverse this to cause a waist in the profile as  $\tau$  increases.

For the free streaming cases, this tendency is reduced due to the initial flow that is present. With initial transverse flow, the energy density of the fireball matter is smeared out into a more radially extended distribution inward from the perimeter to the central regions. Notice from Fig. (2) after the free streaming interval,  $\tau_{eq} - \tau_0$ ,  $\epsilon(\tau_{eq})$  drops much steeper than  $\epsilon(\tau_0)$ , signified by an increasingly negative difference in the percentile profile. At the tail of the distribution, approximately 6 fm in the transverse plane, the percentile profile reverses its slope and gives a positive difference. We see this because the tail of the free streaming energy density distribution, while more dilute, extends farther into the transverse plane, indicating a more subtly increasing distribution. Thus, as the matter cools, the central matter that was compacted into the core with no movement, in the non free streaming case, is now flowing and more evenly distributed towards the outer edges of the fireball, and you obtain a monotonically increasing radius for the freeze-out hypersurface with

no waist.

The freeze-out lifetime of the free streaming fireball occurs around 14.8 fm/c for the initial free streaming from  $\tau_0=0.2$  fm/c to  $\tau_{eq}$ , and 16.2 fm/c for the non free streaming case. The freeze-out hypersurface lifetimes for the different free streaming intervals are similar due to the renormalization scheme we implemented,

$$\epsilon(\tau) = \epsilon(\tau_{eq}) \frac{\tau}{\tau_{eq}} \quad (33)$$

to ensure that the initial entropy distributions at  $\tau_{eq}$ , i.e.  $\frac{ds}{dy}$ , were the same. With similar initial entropy distributions, the lifetime of the fireball would evolve much the same, regardless of the length of the free streaming interval. Although the lifetimes of the fireball were not affected by the interval length of free streaming, the maximum radii assumed a larger value as  $\tau_{eq}$  was increased, again due to the dilution of the initial energy density distribution and a different initial radial velocity profile, by a larger free streaming interval.

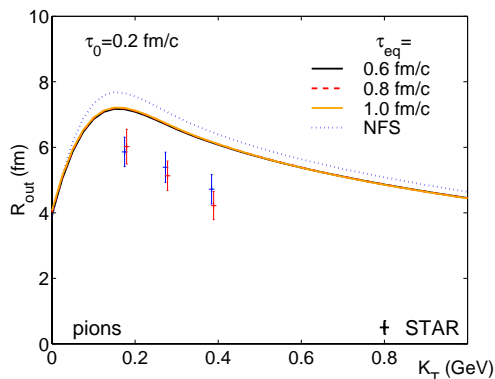


Figure 4: HBT radius  $R_{out}$  with free streaming from  $\tau_0=0.2$ fm/c to  $\tau_{eq}=0.6$ , 0.8 and 1.0 fm/c; also the non free streaming (NFS) case.

The values of the HBT radius  $R_{out}$ , shown in Fig. (4), showed a significant improvement in shifting towards the STAR data. We see a downward shift of 11% in the hydrodynamic predictions with free streaming. The model predictions for the different free streaming intervals are all approximately the same;  $R_{out}$  is related to the lifetime of the fireball, and as explained above the different intervals did not affect the lifetime.

The free streaming modification to the model predictions of  $R_{side}$ , shown in Fig. (5), which corresponds to the radial size of the fireball, were noticeable, but much smaller than the shifts in  $R_{out}$ . With shifts of about 5%, there was little improvement relative to the STAR data which are still larger by 40%. This might seem confusing at first when one compares the difference due the

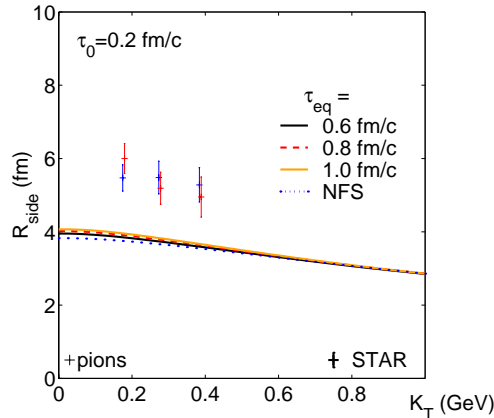


Figure 5: HBT radius  $R_{side}$  with free streaming from  $\tau_0=0.2\text{fm}/c$  to  $\tau_{eq}=0.6$ , 0.8 and 1.0 fm/c; also the non free streaming (NFS) case.

consequence of free streaming of the values for the freeze-out hypersurface radii in Fig. (3) and the values of  $R_{side}$  in Fig. (5); since the high  $p_{\perp}$  particles are emitted from the edges of the fireball, and the low  $p_{\perp}$  particles are emitted from what is initially the core matter of the fireball, and thus smaller radial distance, the high- $p_{\perp}$  particle momenta associated with the larger radii are not represented in Fig. (5).

## 5 Conclusions and Outlook

We have observed that velocity profiles originating from initial free streaming of particles in the early stages of a heavy ion collision have a non negligible effect on the subsequent hydrodynamic evolution and on the final HBT radii. Although this does not completely explain the experimental results gained at RHIC [2], it is a first appreciable refinement of the model to lead to a wider understanding of the collision dynamics and low  $p_{\perp}$  observables. Other groups investigated a more detailed treatment of particle freeze-out, implemented by a hadronic rescattering stage. However it was found that this does not largely alter the HBT observables [10].

In our approach we assume an expansion free of viscosity, and other non-ideal effects. Viscosity would effectively mean a softer equation of state, and therefore even more delayed expansion and cooling, in contrast to the experimental HBT data. On the other hand an equation of state showing a rapid crossover instead of a mixed phase with a rather large thermal heat, as used in our study, could lead to a more drastic expansion [11]. This will be addressed in a forthcoming analysis.

## 6 Acknowledgements

I would like to thank Dr. Ulrich Heinz for his guidance and patience, Peter Kolb for many useful and enlightening discussions, Drs. Lemberger and Palmer for organizing the REU, Ohio State University and the National Science Foundation for funding, the use of the wonderful facilities, and the chance to perform some great research.

## References

- [1] P.F. Kolb, J. Sollfrank, U. Heinz, Phys. Rev. C 62, 054909 (2000).
- [2] C. Adler *et al.* (STAR Collaboration), nucl-ex/0107008; R.C. Johnson *et al.* (PHENIX Collaboration), nucl-ex/0104020;
- [3] J.D. Bjorken, Phys. Rev. D 27, 140 (1983).
- [4] G. Baym, Phys. Lett. B 138, 18 (1984).
- [5] L.D. Landau and E.M. Lifshitz, *Fluid Mechanics* (Pergamon, New York, 1959)
- [6] E. Schnedermann, J. Sollfrank, U. Heinz, Fireball Spectra, Lectures given at NATO Advanced Study Inst. on Particle Production in Highly Excited Matter, Ciocco, Italy, July 12-24, 1992.
- [7] F. Cooper and G. Frye, Phys. Rev. D 10, 186 (1974).
- [8] S. Chapman, and U. Heinz, Phys. Lett. B **340** (1994) 250
- [9] Y.-F. Wu, U. Heinz, B. Tomasik, U.A. Wiedemann, Eur. Phys. J. C1, (1998)
- [10] S. Soff, S. A. Bass, and A. Dumitru, Phys. Rev. Lett 68 (2001) 3981
- [11] D. Zschiesche, S. Schramm, H. Stöcker, and W. Greiner, nucl-th/010737